LARgE survey – III. Environments of ultra-massive passive galaxies at cosmic noon: BCG progenitors growing through mergers

Marcin Sawicki [1,2]*† Liz Arcila-Osejo,[1] Anneya Golob,[1] Thibaud Moutard [1],
Stéphane Arnouts[3] and Gurpreet Kaur Cheema[1]

[1]*Department of Astronomy & Physics and the Institute for Computational Astrophysics, Saint Mary's University, 923 Robie Street, Halifax, Nova Scotia B3H 3C 3, Canada*
[2]*Herzberg Astronomy and Astrophysics, National Research Council of Canada, 5071 West Saanich Rd, Victoria BC V9E 2E7, Canada*
[3]*Laboratoire d'Astrophysique de Marseille, 38 rue Frederic Joliot Curie, Université Aix-Marseille, Marseille F-13388, France*

ABSTRACT

We study the environments of a sample of 61 extremely rare $z \sim 1.6$ Ultra-Massive Passively Evolving Galaxies (UMPEGs: stellar masses $M_\star > 10^{11.5}$ M$_\odot$) which – based on clustering analysis presented in Cheema et al. (2020) – appear to be associated with very massive ($M_{halo} \sim 10^{14.1} h^{-1}$ M$_\odot$) dark matter haloes that are likely to be the progenitors of $z \sim 0$ massive (Coma- and Virgo-like) galaxy clusters. We find that UMPEGs on average have fewer than one satellite galaxy with mass ratio $M_\star^{sat} : M_\star^{UMPEG} \geq 1:5$ (i.e. $M_\star^{sat} \gtrsim 10^{10.8}$ M$_\odot$) within 0.5 Mpc; the large mass gap that we observe between the typical UMPEG and its most massive satellite implies that the $z \sim 1.6$ UMPEGs assembled through major mergers. Using observed satellite counts with merger time-scales from the literature, we estimate the growth rate due to mergers with mass ratio of $\geq 1:4$ to be ~ 13 per cent Gyr^{-1} (with a $\sim 2\times$ systematic uncertainty). This relatively low growth rate is unlikely to significantly affect the shape of the massive end of the stellar mass function, whose evolution must instead be driven by the quenching of new cohorts of ultra-massive star-forming galaxies. However, this growth rate is high enough that, if sustained to $z \sim 0$, the typical $z \sim 1.6$ $M_\star^{UMPEG} = 10^{11.6}$ M$_\odot$ UMPEG can grow into a $M_\star \approx 10^{12}$ M$_\odot$ brightest cluster galaxy (BCG) of a present-day massive galaxy cluster. Our observations favour a scenario in which our UMPEGs are main-branch progenitors of some of the present-day BCGs that have first assembled through major mergers at high redshifts and grown further through (likely minor) merging at later times.

Key words: galaxies: evolution – galaxies: formation – galaxies: high-redshift – galaxies: interactions;.

1 INTRODUCTION

In the modern cosmic structure formation framework, dark matter haloes form from initial density perturbations via gravitational collapse (White & Rees 1978) and subsequently grow bottom-up via hierarchical merging (White & Frenk 1991; Kauffmann & White 1993). Today, the most massive of these haloes host galaxy clusters, at the centres of which reside Brightest Cluster Galaxies (BCGs) – ultra-massive galaxies that are among the most extreme, most massive galaxies in the present-day Universe (stellar masses $M_\star \gtrsim 10^{11.5}$ M$_\odot$, and as high as $\sim 10^{12}$ M$_\odot$; Lidman et al. 2012; Liu, Mao & Meng 2012).

Virtually, all BCGs today are quiescent – i.e. devoid of any significant star formation – with very low specific star formation rates (SSFRs; < SSFR > ~ 0.001 Gyr^{-1}; Fraser-McKelvie, Brown & Pimbblet 2014) that imply (current) mass build-up scales much longer than the present-day age of the Universe. SSFRs in BCGs increase with increasing redshift, so that by $z \sim 1.2$ <SSFR> ~ 0.1 Gyr^{-1} with very few, if any, quiescent examples (McDonald et al. 2016). In agreement with this, models predict that BCG progenitors should be predominantly star forming at high redshifts, $z > 1$, but indicate that a small fraction may have been already massive and quiescent at these early times (Contini et al. 2016). Such Ultra-Massive Passively Evolving Galaxies (UMPEGs; $M_\star > 10^{11.5}$ M$_\odot$), while very rare, have – however – been found at $z > 1$ (e.g. Marchesini et al. 2014; Arcila-Osejo et al. 2019), with a handful of examples spectroscopically confirmed out to $z \sim 4$ (Onodera et al. 2012; Belli, Newman & Ellis 2016; Kado-Fong et al.

2017; Forrest et al. 2020; Stockmann et al. 2020). If they formed as single objects through intense bursts of star formation, UMPEG progenitors must have had SFRs of several hundred $M_\odot$ yr^{-1} (e.g. Arcila-Osejo et al. 2019). Moreover, UMPEGs are very strongly clustered (Cheema et al. 2020), suggesting that they are associated with the high-z progenitors of present-day massive galaxy clusters; UMPEGs could therefore be the direct, main-branch progenitors of some of the present-day BCGs. Altogether, UMPEGs appear to be extreme examples among the high-z galaxy population; because they are so extreme, they provide a unique opportunity to test our understanding of galaxy formation and evolution in the extreme regions of galactic parameter space that these monster galaxies occupy.

Simulations (e.g. De Lucia & Blaizot 2007; Ragone-Figueroa et al. 2018) predict that a main-branch BCG progenitor (whether star forming or quiescent) is often already well established by $z \sim 1.5$ and contains 10–30 per cent of the BCG's present-day stellar mass by that redshift. Major mergers can be expected to play an important role in the formation of these ultra-massive galaxies (UMGs) because of dynamical friction (Ostriker & Tremaine 1975), whose effect increases with increasing satellite mass (Chandrasekhar 1943). As a result, massive galaxies at the core of their dark matter halo can be expected to merge relatively quickly to form an even more luminous and massive galaxy, leaving as evidence of such merging a substantial luminosity gap between the brightest and second-brightest galaxy in the system (Ostriker & Tremaine 1975; Jones, Ponman & Forbes 2000; Tal et al. 2012). The more detailed semi-analytic formation models (e.g. De Lucia & Blaizot 2007; Contini et al. 2016) indeed predict a significant major-merger phase, expected to occur at high redshift ($z > 1$), although *in situ* star formation (before quenching occurs) and minor mergers can also contribute to the growth.

At low and intermediate ($z \lesssim 1$) redshifts, observations suggest that mergers continue to add mass to the BCGs (e.g. Edwards & Patton 2012; Liu et al. 2012, 2015; Burke & Collins 2013; Lidman et al. 2013). However, to test the merger paradigm at high redshifts, $z \gtrsim 1$, requires first the ability to identify high-z BCG progenitors. Such progenitor identification is non-trivial given that – as mentioned earlier – the progenitors are expected to evolve substantially through mergers (as required by the model).

One way to proceed is to modify the abundance-matching technique by correcting for the effects of merging using predictions from numerical simulations (e.g. Marchesini et al. 2014; Vulcani et al. 2016; Cooke et al. 2019). These studies report the detection of a significant number of UMG progenitors at high redshift, $z \gtrsim 1$, and find that while many of them are star forming, a non-negligible fraction is already quenched. At $1 \lesssim z \lesssim 2$, growth in UMG stellar masses comes from a combination of *in situ* star formation, which is estimated directly from observational data, and from mergers, whose effect is estimated from simulations (Cooke et al. 2019). While supporting the importance of mergers at high redshift, this approach does not test it directly as it uses hierarchical halo merger models to both help identify BCG progenitors and to estimate merger and mass growth rates (Cooke et al. 2019). Merger rates can instead be more directly estimated from the data by counting the incidence of close companions or disturbed morphologies, as done by Vulcani et al. (2016) and Zhao et al. (2017), who find evidence for mergers at $z > 1$, although still relying on abundance matching for progenitor identification.

An alternative approach to testing the merger scenario is to identify BCG progenitors in a way that is less dependent on assumptions inherent in galaxy abundance matching, whether corrected or not

using hierarchical merger trees. In Arcila-Osejo et al. (2019), we used wide area imaging to identify a population of $z \sim 1.6$ UMPEGs, and their extremely strong clustering ($r_0 = 29.77 \pm 2.75\,h^{-1}$Mpc) suggests that they are associated with haloes of mass $M_{halo} \sim 10^{14.1} h^{-1}M_\odot$ (Cheema et al. 2020). Under the assumption of smooth halo-mass growth, these $z \sim 1.6$ haloes are likely to be the progenitors of present-day massive ($M_{halo} \sim 10^{15}M_\odot$) galaxy clusters (Cheema et al. 2020). While only approximately one out of eight of such massive $z \sim 1.6$ haloes appear to contain an UMPEG (the remaining haloes presumably contain star-forming UMGs, or collections of lower mass pre-merger components), the very high stellar masses of our UMPEGs and their very strong clustering suggest that UMPEGs are direct, main-branch progenitors of some of the present-day BCGs in massive clusters. These $z \sim 1.6$ objects thus provide a sample of plausible proto-BCGs with which to test the BCG hierarchical growth scenario at high redshift.

In this paper, we will examine the environments of these $z \sim 1.6$ BCG progenitors. The depth of our data set is not sufficient over most of its area to find normal, sub-M^*, galaxies around them, and consequently, we are not in a position to see directly if they reside at centres of (proto)clusters. Instead, we will search for evidence of major mergers in the formation and growth of our UMPEGs. We will do so not by searching for merger signatures such as disturbed morphologies or tidal features (e.g. Patton et al. 2000; Lotz et al. 2008; Bridge, Carlberg & Sullivan 2010), as our data are also too shallow to detect such low-surface-brightness features at $z \sim 1.6$. Instead, we will search for (relatively) massive companions that represent a reservoir of material for future mergers. The number of such massive companions, combined with dynamical friction time-scales, will give us an estimate of the mass growth due to mergers. At the same time, the presence of a significant mass (or luminosity) gap between the UMPEGs and their most massive (or luminous) satellites will provide evidence that major mergers have already happened.

Throughout this work, we use the AB magnitude system (Oke 1974) and assume the Chabrier (2003) stellar initial mass function (IMF) when calculating stellar masses of galaxies. We adopt the flat Λ cosmology with $\Omega_{m,0} = 0.3$, $\Omega_{\Lambda,0} = 0.7$, and Hubble constant of $H_0 = 70$ km s^{-1}Mpc^{-1}. In this cosmology, 1 Mpc (physical) corresponds to 118.0 arcsec, or $\sim$2 arcmin, at $z \sim 1.6$ (Wright 2006).

2 DATA AND SAMPLE SELECTION

The detailed description of our catalogues and sample selection is given in Arcila-Osejo et al. (2019), so here we only summarize the key details.

We selected $z \sim 1.6$ galaxies using an adaptation of the Daddi et al. (2004) BzK technique developed by Arcila-Osejo & Sawicki (2013). This 'gzK_s technique' selects $z \sim 1.6$ star-forming (SF-gzK_s) and passively evolving (PE-gzK_s) galaxies using a combination of optical and near-IR photometry. For the optical data, we used the g and z images from the T0006 release of the CFHT Legacy Survey (CFHTLS; Goranova et al. 2010), specifically all four of its Deep fields (D1, D2, D3, and D4), and two of the Wide fields (W1 and W4). For the NIR data in W1 and W4, we used the K_s images from the Visible Multi-Object Spectrograph (VIMOS) Public Extragalactic K_s Survey Multi-Lambda Survey (VIPERS-MLS; Moutard et al. 2016a); meanwhile, in the Deep fields we used the K_s and H-band data from the T0002 release of the WIRCam Deep Survey (WIRDS; Bielby et al. 2012).

Requiring overlap between the optical and NIR data sets, and after masking areas around bright stars, low-SNR regions, and

other artefacts, our data cover 25.09 deg^2 in the two Wide fields and 2.51 deg^2 in the Deep fields, giving a total area of 27.6 deg^2. In the wide fields, we reach 90 per cent detection completeness at $K_s = 20.5$ AB; in the Deep D1, D3, and D4 fields, we reach 50 per cent detection completeness at $K_s = 23.5$ AB, while in D2 (the COSMOS field) we reach it at $K_s = 23.0$ AB.

We used SEXTRACTOR (Bertin & Arnouts 1996) to perform object detection in the K_s band and then matched-aperture photometry in other bands. Applying the gzK_s selection technique of Arcila-Osejo & Sawicki (2013) to these data gave us 8756 gzK_s galaxies with $19.25 < K_s < 20.25$ in the Wide fields and 53 988–65 586 (the lower number is for secure $z \sim 1.6$ galaxies and the upper number includes some possible lower z interlopers) with $19.25 < K_s < 23.5$ in the Deep fields. Comparison of our sample in the COSMOS (CFHTLS D2) field with the catalogue of Muzzin et al. (2013b) shows that gzK_s galaxy redshift distributions very with type (*PE-gzK$_s$* and *SF-gzK$_s$*) and magnitude: the peak is at $z \sim 1.5$ for the brightest galaxies and shifts to $z \sim 1.7$ for fainter galaxies ($K_s \sim 22$–23), while the full width at half-maximum (FWHM) of the distribution is ~ 0.8 for *PE-gzK$_s$* galaxies and ~ 1.1 for *SF-gzK$_s$* (see fig. 6 of Arcila-Osejo et al. 2019 for an illustration).

The brightest among the *PE-gzK$_s$* galaxies is of special interest. In order to be already quiescent at $z \sim 1.6$ and yet very bright in the NIR suggests that they must be very massive and thus must have formed under extreme conditions at even higher redshifts. We thus defined in Arcila-Osejo et al. (2019) a sample of UMPEGs to be *PE-gzK$_s$* galaxies with $K_s < 19.5$. This selection corresponds to quiescent galaxies with stellar masses $M_\star \gtrsim 10^{11.5} M_\odot$, and with mean stellar mass $\langle M_\star \rangle = 10^{11.6} M_\odot$. Our sample of UMPEGs consists of 61 objects, the vast majority (all but six) located in the two Wide fields (W1 and W4). For full details of the object detection, photometry, UMPEG selection, and stellar mass estimation, please see Arcila-Osejo et al. (2019).

3 SATELLITE COUNTS

Haloes of mass $\sim 10^{13} M_\odot$ are expected to have virial radii of 0.5 Mpc at $z \sim 1.6$ (Munoz-Cuartas et al. 2011). Our clustering analysis suggests that our $z \sim 1.6$ UMPEGs reside in haloes that are an order of magnitude more massive (Cheema et al. 2020), so searching for potential satellite galaxies within a 0.5 Mpc radius seems justified, as it is likely to yield a physically associated population. We perform this search by conducting a census of all gzK_s galaxies located in 0.5 Mpc (projected) proximity to each UMPEG followed by a statistical correction to account for contamination due to chance projections.

Fig. 1 shows our census of the potential satellites of our UMPEGs in the Wide (top panel) and Deep (bottom panel) fields. The rest-frame i-band luminosities of the UMPEGs, derived from their K_s magnitudes, are shown on the horizontal axes, while the vertical axes show the i-band luminosity ratios (L_{comp}/L_{UMPEG}) for the (potential) satellites. The candidate satellites in Fig. 1 include physically unassociated gzK_s fore/background galaxies, so the number of objects shown can be regarded as an upper limit on the number of physically associated companions. However, even with this simple analysis it is clear that UMPEGs have extremely few luminous companions: of the 61 UMPEGs in our sample, only four have a companion with luminosity ratio $L_{comp}/L_{UMPEG} > 0.5$ (objects above the dashed line). Only at $L_{comp}/L_{UMPEG} < 0.2$ do we start seeing significant numbers of companions, although many of these are likely to be physically unassociated chance projections.
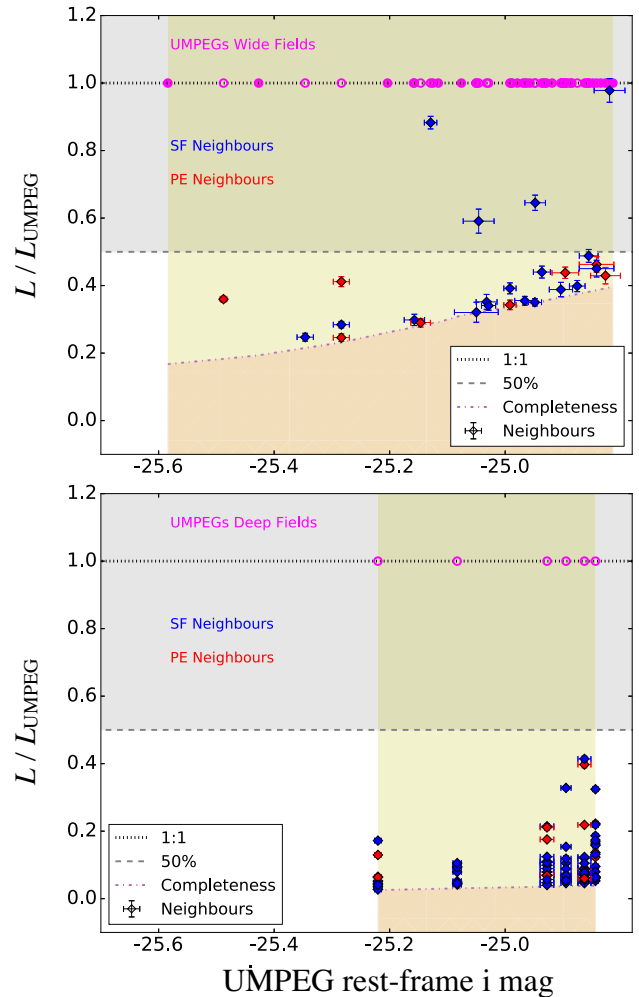

Figure 1. Satellite galaxy candidates. Luminosity ratios (satellite candidate compared to that of its UMPEG) are plotted as function of UMPEG luminosity in rest-frame i band. The top panel shows data in the Wide fields, and the bottom panel is for the Deep. The yellow area shows the magnitude range of our UMPEGs; open magenta symbols identify UMPEGs with satellite candidates, whereas filled magenta points are for UMPEGs with no satellites. The grey shaded area represents the positions these companions would occupy if they were at least 50 per cent as bright as the central UMPEG. The completeness limit for each sample, reported in Section 2, is shown with a dot–dashed line.

Of course, we currently have no way of individually identifying which of the objects in Fig. 1 are physically associated with our UMPEGs and which are chance projections. We can, however, statistically correct for this foreground/background contamination using the well-established approach recently employed by a number of studies that characterize the satellite galaxy populations around massive galaxies (e.g. Tal et al. 2012; Tal et al. 2013; Kawinwanichakij et al. 2014; Hartley et al. 2015; Chen et al. in preparation). In this approach, the (fore/background-contaminated) number counts of galaxies within a projected cylinder centred on the central galaxy are corrected by subtracting the magnitude-dependent number counts inferred from similar cylinders placed at random positions in the survey area. In our case, to compute the background we randomly place within our survey area three hundred apertures with radius 0.5 Mpc each (ensuring that they do not overlap with the 0.5 Mpc apertures centred on our UMPEGs),

and then count gzK_s galaxies within them to arrive at the background number density as function of magnitude and galaxy type (PE-gzK_s or SF-gzK_s). Subtracting these numbers from the counts of gzK_s galaxies around the UMPEGs statistically removes physically unassociated, projected foreground/background gzK_s galaxies: this correction statistically deems most UMPEG companions in the Wide fields as unphysical, and ∼60 per cent in the Deep fields. Applying this correction gives us the background-corrected observed surface density of true, physically associated satellites, Σ_{obs}.

We next need to correct for an additional source of incompleteness that affects the probability of detecting satellites. Here, we note that the redshift distribution of UMPEGs is approximately Gaussian-shaped (Arcila-Osejo et al. 2019) and that this is a reflection of the gzK_s selection window rather than a real physical decrease in the abundance of ultra-massive galaxies away from z ∼1.6. This means that objects whose redshifts are away from the peak of the redshift distribution have a reduced probability of detection. This effect affects the detectability of UMPEGs, but because we do not analyse the environments of such undetected UMPEGs, our satellite statistics are not affected. However, the detectability of satellites UMPEGs that *are* detected but are at redshifts offset from the peak of the redshift distribution is also reduced, and we need to account for these undetected satellites. We correct for this incompleteness by statistically weighing Σ_{obs} as

$$\Sigma_{true} = \Sigma_{obs} \times \frac{\int N_{UMPEG}(z)dz}{\int N_{UMPEG}(z) \times N_{comp}(z)dz}, \qquad (1)$$

where Σ_{true} represents the true surface density of satellites, corrected for both fore/background galaxies, and satellite detection completeness. The $N(z)$ are the redshift probability distributions of UMPEGs or companions. For these redshift distributions, we adopt the photometric redshift distributions shown in Fig. 6 of Arcila-Osejo et al. (2019), noting that the probability density distribution $N(z)$ is different for UMPEGs and companions given their different K_s magnitudes and the fact that companions can be star forming or passive. In equation (1), the denominator accounts for the fact that companions will only be detected when both their central UMPEGs *and* they themselves are detected, and this is proportional to both the UMPEG and companion detection probabilities; the numerator accounts for the redshift-dependent detection probability of the UMPEGs.

Fig. 2 shows the results of applying this procedure, binned in bins of luminosity ratio and separated for SF-gzK_s and PE-gzK_s satellites. The grey curve shows the cumulative number density of satellites (of both types) summed starting with the most luminous. Note that in this figure we have converted the observed quantities (number per arcmin²) into physical ones (number per Mpc²) using our adopted cosmology.

It is clear in Fig. 2 that UMPEGs have virtually no physically associated satellites with $L/L_{UMPEG} \gtrsim 0.5$, and even summing down to $L/L_{UMPEG} \sim 0.25$ there is only on average one satellite per UMPEG. The shape of the distribution, with its low number of luminous satellites followed by an increase in satellite number at lower masses, is reminiscent of the 'gap' reported by Tal et al. (2012) in the luminosity function of z ∼0.3–0.7 distant red galaxies (DRGs). The details of their distributions are not directly comparable to those of ours because we normalized our satellite UMPEG luminosities, whereas Tal et al. (2012) left heir DRG luminosities un-normalized. Nevertheless, the size of the luminosity gap – which Tal et al. defined as the point at which the cumulative satellite distribution reaches one satellite per central – is similar: in
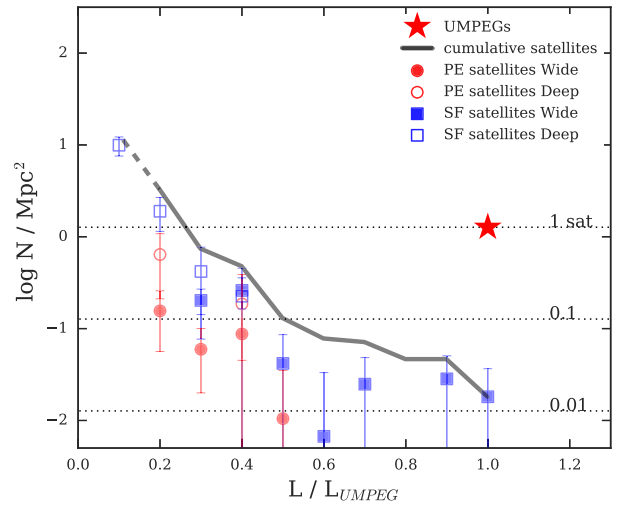

Figure 2. The background-subtracted surface number density of companions within 0.5 Mpc of UMPEGs as a function of rest-frame i-band luminosity ratio. The three dotted horizontal lines show (top to bottom) 1, 0.1, and 0.01 satellites per UMPEG. The black curve shows the cumulative number density of satellites: solid where we are complete and dashed to indicate the lower limit where we do not detect PE-gzK_s galaxies. It is clear that UMPEGs lack companions of comparable luminosity even in this figure, which does not remove unassociated fore/background projections. Even at luminosities ∼0.2 × L_{UMPEG}, there is only one companion (physical + projected) per UMPEG.

their DRG sample they found it to be $L_{sat}/L_{DRG} \sim 0.3$, which is similar to the $L_{sat}/L_{UMPEG} \sim 0.25$ that we find for our UMPEGs. The implications for our z ∼1.6 UMPEGs are similar to those for the intermediate-redshift DRGs of Tal et al.: the paucity of luminous companions suggests that our UMPEGs may have formed a significant time before the redshift of observation – z ∼1.6 in our case – and that their subsequent growth will be moderate and mainly through minor mergers. We will expand on these points in Section 4.

4 DISCUSSION

4.1 Masses of UMPEG satellites

UMPEGs are already extremely massive ($M_\star^{UMPEG} > 10^{11.5} M_\odot$), but it is interesting to consider how much they could grow by absorbing their satellites, as these lose momentum via dynamical friction and in-spiral towards the centre of the host dark matter halo. To do so, we first need to estimate the stellar masses of the satellites before we estimate how quickly these satellites will merge with their UMPEGs.

In Arcila-Osejo et al. (2019), we determined an empirical K_s–$M_\star$ relation for quiescent galaxies by matching our K_s magnitudes of PE–gzK_s galaxies in the COSMOS field with their stellar masses from the Muzzin et al. (2013b) catalogue that's based on SED fitting of multiband photometry. Fitting the resulting distribution gave us the relation

$$\log[M_\star^{PEG}/M_\odot] = -0.348 K_s + 18.284, \qquad (2)$$

which we can apply to the quiescent satellites. Because many of the satellites are star forming, we also need a similar relation for SF-gzK_s and so we now repeat the above matching but for SF-gzK_s galaxies and show the results in Fig. 3, where the magnitudes are our total K_s magnitudes, the stellar masses are again from the catalogue
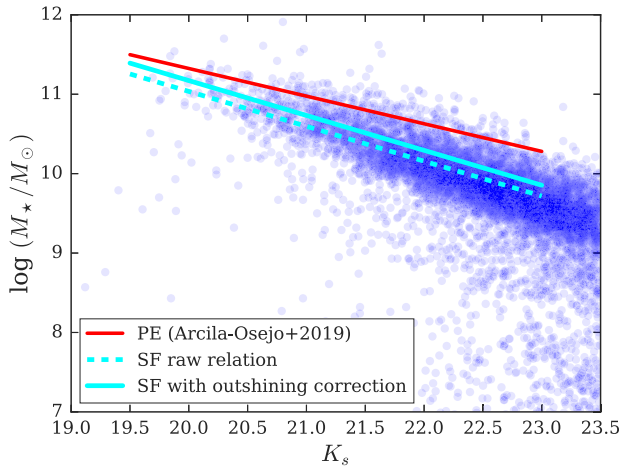
Figure 3. The mass–magnitude relation for star-forming gzK_s galaxies in the COSMOS field. The dashed blue line is a fit to the data as they are, while the solid blue line represents that raw relation adjusted for the effects of outshining in stellar mass estimates following the empirical prescription of Sorba & Sawicki (2018). The red line shows the mass–magnitude relation for quiescent, PE-gzK_s galaxies from Arcila-Osejo et al. (2019).

of Muzzin et al. (2013b), and the dashed blue line shows the line of best fit to these data. Note, however, that there is growing evidence that spatially unresolved spectral energy distribution (SED) fitting (such as that in Muzzin et al. 2013b but also in the vast majority of other studies) underestimates stellar masses of star-forming galaxies (Sorba & Sawicki 2018; see also Zibetti, Charlot & Rix 2009; Sorba & Sawicki 2015; Abdurro'uf & Akiyama 2018). The effect arises because old stars, which can contain the bulk of a galaxy's stellar mass, are masked in broad-band photometry that is used in SED fitting by much brighter but less numerous young stars (Sorba & Sawicki 2015, 2018; see also Sawicki & Yee 1998). As shown in Sorba & Sawicki (2015) and Sorba & Sawicki (2018), this systematic mass underestimate depends on specific star formation rate (SSFR) and so we correct the raw best-fitting relation (dashed line in Fig. 3), using the prescription from Sorba & Sawicki (2018, their equation 6) taking SSFR $= 10^{-8.8}$ yr^{-1}, as appropriate for high-mass ($M_\star \sim 10^{10}$ M$_\odot$) star-forming galaxies at $z \sim 1.6$ (Whitaker et al. 2014; Johnston et al. 2015). The result is an increase of star-forming galaxy stellar masses by $\Delta M_\star^{\rm SFG} = 37$ per cent on average, as compared to the masses from spatially unresolved SED fits. The resulting mass–magnitude relation, corrected for the outshining effect, is then given by

$$\log[M_\star^{\rm SFG}/{\rm M}_\odot] = -0.439 K_s + 19.958, \tag{3}$$

and is shown with the solid cyan line in Fig. 3. The relation for quiescent galaxies (equation 2) is shown with the red line for reference.

Using the K_s–$M_\star$ relations for quiescent (equation 2) and star-forming (equation 3) galaxies, and assuming that UMPEGs have a mass of $M_\star^{\rm UMPEG} = 10^{11.57}M_\odot$ (the mean mass of our UMPEG sample), we recast the data of Fig. 2 in terms of stellar masses. The result is plotted in Fig. 4. As that figure shows, on average, UMPEGs have virtually no massive physical companion galaxies (mass ratios $M_\star^{\rm sat} : M_\star^{\rm UMPEG} \gtrsim$ 1:3). One has to integrate down to $M_\star^{\rm sat} : M_\star^{\rm UMPEG} \approx$ 1:5.5 to find one satellite per UMPEG, on average.

We note that for a typical UMPEG with $M_\star^{\rm UMPEG} \approx 10^{11.6}M_\odot$, satellites of 1:5.5 mass ratio have stellar masses
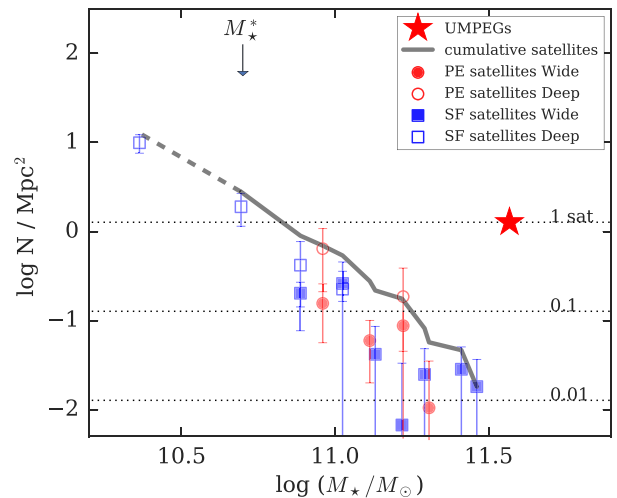

Figure 4. The background-subtracted surface number density of satellites within 0.5 Mpc of UMPEGs as a function of stellar mass. The black curve shows the cumulative number density of satellites: solid where we are complete and dashed to indicate the lower limit where we do not detect PE-gzK_s galaxies. The three dotted horizontal lines show (top to bottom) 1, 0.1, and 0.01 satellites per UMPEG. The location of the characteristic Schechter mass, $M_\star^*$, is indicated.

$M_\star^{\rm sat} = 0.18 \times M_\star^{\rm UMPEG} \approx 10^{10.8}$, which is similar to the characteristic Schechter mass of $M_\star^* \sim 10^{10.6-10.8}$ for quiescent $z \sim 1.6$ galaxies (indicated with the arrow in Fig. 4; Arcila-Osejo & Sawicki 2013; Ilbert et al. 2013; Muzzin et al. 2013a; Tomczak et al. 2014; Arcila-Osejo et al. 2019). Consequently, our 'low-mass' UMPEG satellites are in fact very massive themselves. Nevertheless, in relative terms, they are of significantly lower mass than the mass of the UMPEGs that they are associated with and with which they will likely eventually merge.

We will consider how mergers – both minor and major – contribute to the growth of UMPEGs in the next section.

4.2 UMPEG growth through mergers

4.2.1 Growth rate estimate

It is interesting to consider how much (or how little) UMPEG masses can grow by absorbing stellar material from the galaxies we observe in their environment. For this, consider Fig. 5 that shows the stellar mass surface density in satellites out to our 0.5 Mpc search radius. The black line shows the cumulative surface stellar mass density contributed by the satellites and it is clear that the sum of the masses of all major satellites of UMPEGs is quite small: for example, down to $M_\star^{\rm sat} = 10^{11.0}$ M$_\odot \approx 0.25 \times M_\star^{\rm UMPEG}$, the stellar masses of all the satellites add up just under a quarter the mass of the central UMPEG; down to $M_\star^{\rm sat} = M_\star^* = 10^{10.7}M_\odot$, the mass contained in satellites is only $\sim$40 per cent times the mass of the UMPEG. Clearly, there is not a lot of stellar material available for growth via major ($M_\star : M_\star^{\rm UMPEG} >$ 1:4) mergers in the vicinity of the UMPEGs.

We can make a rough estimate of the mass accretion rate, for which we need a merger timescale. First, we make a crude estimate of the merger time-scale, $T_{\rm merge}$, using the dynamical friction formula from Jiang et al. (2008, their equation 8). We assume a value of $\varepsilon = 0.5$, which is independent of the masses of the interacting
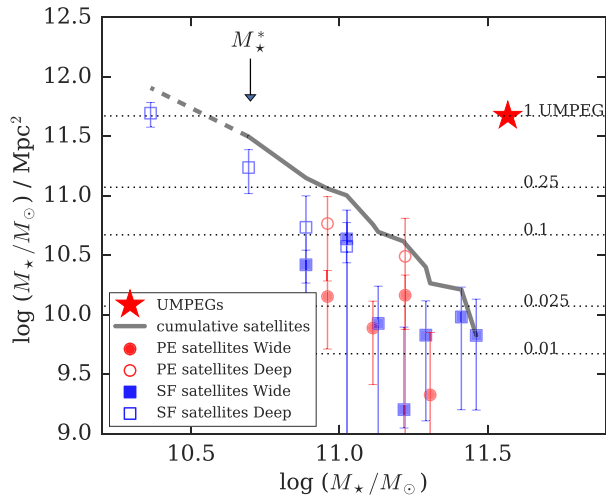
Figure 5. The background-subtracted surface mass density of satellites within 0.5 Mpc of UMPEGs as a function of stellar mass. The black curve shows the cumulative number density of satellites: solid where we are complete and dashed to indicate the lower limit where we do not detect $PE–gzK_s$ galaxies. The location of the characteristic Schechter mass, $M_\star^*$, is indicated. The dotted horizontal lines show (top to bottom) 1, 0.25, 0.1, 0.025, and 0.01 times the mass density of a typical ($M_\star = 10^{11.57} M_\odot$) UMPEG if that mass were distributed over the same projected area as the mass contained in the satellites.

galaxies (Jiang et al. 2008), and circular velocity $v \sim 860$ km s^{-1} (a velocity that relates to a high likelihood of interaction for close pairs; Patton et al. 2000). We also estimate T_{merge} using the formula from Kitzbichler & White (2008, their equation for $\Delta v < 3000$ km s^{-1}) that is calibrated for close pairs but does provide an estimate of T_{merge} alternative to that of Jiang et al. (2008).

Applying the two T_{merge} estimators to the UMPEG companions and summing over the sample after appropriately weighting by the fore/background counts allows us to estimate the merger time-scales, and then – incorporating our satellite mass estimates – to arrive at the mass accretion rates. The two merger time-scale prescriptions yield accretion rates that are consistent for high-mass satellites but differ by up to a factor of ∼2 at lower $M_\star^{sat}$. Taking the average of the two gives a growth rate of ∼13 per cent Gyr^{-1} for an UMPEG with $M_\star^{UMPEG} = 10^{11.6} M_\odot$, with an uncertainty of a factor of 2 that is driven by the systematic uncertainty in the T_{merge} estimate.

4.2.2 Growth since z ∼1.6

While we do not know whether the accretion rate remains constant for UMPEGs, there are indications for lower mass central galaxies that satellites that are consumed are almost exactly replenished by new arrivals from beyond the halo (Tal et al. 2013; Hartley et al. 2015). It thus seems plausible that newly arriving satellites keep the UMPEG haloes stocked with new arrivals as existing satellites sink towards the halo's centre due to dynamical friction and are consumed by merging with the UMPEGs. Taking the estimated growth rate of ∼13 per cent Gyr^{-1} at face value would grow our fiducial UMPEG from $M_\star^{UMPEG} = 10^{11.6}$ M$_\odot$ at $z \sim 1.6$ to $M_\star^{z=0} = 10^{11.9–12.1}$ M$_\odot$ by $z \sim 0$ (the mass range reflects linear or exponential growth in the accretion rate). Notably, this forecast $z \sim 0$ UMPEG mass is comparable to the masses of BCGs in present-day massive galaxy clusters ($M_\star \sim 10^{11.7}$ M$_\odot$ with a few

examples at $M_\star > 10^{12}$ M$_\odot$; see compilation by Lidman et al. 2012). For example, the mass of NGC 4874 (one of the central galaxies of the Coma cluster) is $M_\star \sim 10^{12.0}$ (Veale et al. 2017).

Our mass growth calculation is crude, as it assumes a constant merger rate (whereas – at least for lower-mass galaxies – merger rates decrease with time; e.g. Patton et al. 2002; Bridge et al. 2010) and, moreover, does not account for accretion of low-mass satellites or for possible re-ignition of star formation in the UMPEGs. However, this rough calculation does yield a projected $z \sim 0$ UMPEG mass that is consistent with the masses of massive cluster BCGs at $z \sim 0$ and thereby with the idea, first suggested on the basis of clustering measurements in Cheema et al. (2020), that our $z \sim 1.6$ UMPEGs are the direct progenitors of some of the central BCGs of massive present-day galaxy clusters.

Our mass growth rate estimate appears to be somewhat higher than that reported by Vulcani et al. (2016), who used the modified galaxy abundance-matching method of Marchesini et al. (2014) to select the progenitors of massive ($M_\star > 10^{11.8}$ M$_\odot$) $z \sim 0$ galaxies at earlier epochs and then used counts of their satellites to infer merger mass growth. Vulcani et al. report that a present-day $M_\star \gtrsim 10^{11.8}$ massive galaxy progenitor, which in their abundance-matching selection has a typical $z \sim 1.7$ mass of $M_\star \sim 10^{11.35}$, can only reach its final mass through a combination of mergers and *in situ* star formation (roughly half of their progenitors are star forming at $1.5 \gtrsim z \gtrsim 2$). This would appear at odds with our conclusion, but we note some important differences between the two studies: First, our UMPEGs are selected via clustering, rather than through galaxy abundance matching, so they may represent a different population; this, and the fact that our UMPEGs are selected to be quiescent – while the Vulcani et al. objects include a large number of star-forming systems – suggests that UMPEGs could be preferentially older systems, likely located in regions that collapsed earlier in the history of the Universe than those that host the typical object in the Vulcani et al. sample. Secondly, our UMPEGs are more massive than the Vulcani et al. objects, which means they require less mass growth to reach the same final $z \sim 0$ mass. And third, it is likely that the masses of the star-forming (albeit not quiescent) galaxies in the Vulcani et al. sample are underestimated (Sorba & Sawicki 2018, and Section 4.1); accounting for this underestimate would make more satellite mass available for merging, making growth through mergers more efficient than estimated by Vulcani et al.; furthermore, the mass bias would also make the star-forming centrals in the Vulcani et al. more massive, making it even easier for them to reach the target $z \sim 0$ mass. For these reasons, and also because our mass growth estimates are rather crude (as discussed earlier), we do not feel that the results of the two studies are in conflict. On the contrary, given the systematic effects discussed above, the results may give a consistent picture in which the $z \sim 1.6$ quiescent progenitors of present-day massive centrals grow through mergers alone, while their star-forming progenitors grow through a combination of mergers and (until quenched) *in situ* star formation.

As a final point in this section we briefly discuss the effect of mergers on the evolution of the massive end of the stellar mass function. The relatively low-mass growth rate from mergers that we estimate suggests that the evolution of the massive end of the stellar mass function of quiescent galaxies is not strongly affected by mergers. Instead, the growth seen from $z \sim 1.6$ to intermediate and low redshifts (Arcila-Osejo & Sawicki 2013; Muzzin et al. 2013a; Ilbert et al. 2013; Moutard et al. 2016b; Arcila-Osejo et al. 2019) must be primarily driven by the arrival of newly quenched massive galaxies joining the quiescent population.

4.2.3 Growth before z ~1.6

It is also interesting to consider how our $z \sim 1.6$ UMPEGs may have grown from higher redshift progenitors, and a clue lies in the presence of the gap – noted in Section 3 – between the mass (or luminosity) of the UMPEG and the mass (or luminosity) of its most massive (luminous) companion. In terms of luminosity, the gap is $L_{\rm 1st\,sat}/L_{\rm UMPEG} \sim 0.25$ (i.e. $\sim$1.5 mag), and is of similar size to the luminosity gap found for satellites of massive quiescent DRGs at $z = 0.3$–0.7 by Tal et al. (2012) ($L_{\rm 1st\,sat}/L_{\rm DRG} \sim 0.3$). For our $z \sim 1.6$ UMPEGs, the gap in mass is $M_\star^{\rm 1st\,sat}/M_\star^{\rm UMPEG} \sim 5.5$ (Fig. 4).

The presence of a significant luminosity gap between the first and second most luminous group members can be interpreted as indicative of the age of the hosting environment (e.g. Tremaine & Richstone 1977; Milosavljević et al. 2006; Van Den Bosch et al. 2007; Dariush et al. 2010; Raouf et al. 2018). This is because the most massive group members, which are the ones most strongly affected by dynamical friction, can be expected to merge rapidly, leaving behind only the less-massive satellites as these suffer less deceleration due to dynamical friction. Major mergers thus provide a natural explanation for the presence of the luminosity (and mass) gap in our UMPEG environments.

Further evidence for this scenario is provided by the fact that about 10 per cent of our original UMPEG candidates, excluded from the sample, appear to be double-cored systems (see Arcila-Osejo et al. 2019). These systems may be late-stage mergers of pairs of massive and already-quiescent UMPEG building blocks (so-called dry mergers). Of course, mergers that build UMPEGs might also be wet (i.e. gas rich and resulting in additional star formation), but we have no immediate way of observationally linking our UMPEGs to such wet merger progenitors with the present data. We note that our UMPEGs cluster extremely strongly (see Cheema et al. 2020) – much more strongly that do potential high-z massive wet merger candidates such as sub-millimetre galaxies (SMGs; e.g. Blain et al. 2004; Hickox et al. 2012; Wilkinson et al. 2017) or dust obscured galaxies (DOGs; e.g. Brodwin et al. 2008; Toba et al. 2017). It therefore seems that UMPEGs are associated with more massive, rarer dark matter haloes than is typical of high-z starbursts. This clustering argument does not rule out the possibility of wet mergers as UMPEG progenitors, but it does suggest that if SMGs and DOGs are wet mergers, the majority of them are not the wet mergers that later quenched to become UMPEGs.

It is also interesting to consider if the mass accretion rate we estimated in Section 4.2.2 is consistent with the major merger scenario. By construction, this merger rate estimate is for major mergers ($M:M_\star^{\rm UMPEG} = 1:4$). Applying the $\sim$13 per cent Gyr^{-1} estimated growth rate to our fiducial $M_\star^{\rm UMPEG} = 10^{11.57} {\rm M}_\odot$ galaxy, and assuming for simplicity that major mergers are the only mass growth mechanism, we get a $z = 4$ mass of $M_\star = 10^{11.43} {\rm M}_\odot$ (given the short time-span between $z = 4$ and $z = 1.6$, the numbers are almost the same for linear and exponential growth and so we took the average of the two here). This growth could, for example, be accomplished through a single $\sim$3:1 merger ($10^{11.43} {\rm M}_\odot$ + $10^{11.00} {\rm M}_\odot \rightarrow 10^{11.57} {\rm M}_\odot$). In this context, it is interesting to note again that $\sim$10 per cent of our initial UMPEG candidates in Arcila-Osejo et al. (2019) were rejected when visual inspection revealed them to have two sub-$M^{\rm UMPEG}$ components; these rejected candidates could represent ongoing major mergers that will coalesce into UMPEGs over time, consistent with the major-merger scenario of UMPEG growth.

Finally, the inferred $z \sim 4$ mass of $M_{\rm UMPEG}^{z=4} = 10^{11.43} {\rm M}_\odot$ can also be compared with the masses of the photometrically selected $z \sim 4$ quiescent galaxies of Kubo et al. (2018, $M_\star = 10^{11.02-11.26} {\rm M}_\odot$), or with the masses of the most extreme, spectroscopically confirmed examples ($M_\star = 10^{11.23} {\rm M}_\odot$; Glazebrook et al. 2017; $M_\star = 10^{11.49} {\rm M}_\odot$, Forrest et al. 2020). Most of these masses are somewhat lower than those of our projected UMPEG progenitors, but not dramatically so, and so it could be expected that significant numbers of high-mass $z \sim 4$ quiescent galaxies would be found in larger-area surveys. It seems that these observed $z \sim 4$ quiescent galaxies could potentially grow into $z \sim 1.6$ UMPEGs, and then $z \sim 0$ BCGs, through a combination of major and minor mergers. In this context, we note that Kubo et al. (2018) present evidence for the growth of $z \sim 4$ massive galaxies through minor mergers, while Shi et al. (2019) report a significant number of massive ($M_\star > 10^{11} {\rm M}_\odot$) quiescent galaxy candidates in a $z \sim 4$ protocluster that they interpret as the central galaxies of massive (sub)haloes that one could expect to merge as the protocluster coalesces. In further agreement with this scenario, Marsan et al. (2019) and Stockmann et al. (2020) report that many of their ultramassive quiescent galaxies at $z \sim 1.5$–2.5 show signs of interactions and mergers.

Overall, the arguments we presented suggest a scenario in which galaxies that follow the UMPEG evolutionary pathway may grow through major mergers at very high redshifts, $z > 1.6$, before being observed as quiescent UMPEGs at $z \sim 1.6$, and then growing mildly mostly through minor mergers at lower redshifts.

5 CONCLUSIONS

In this paper, we examined the environments of 61 ultra-massive ($M_\star > 10^{11.5} {\rm M}_\odot$) galaxies that were already quiescent by $z \sim 1.6$ – i.e. near the peak epoch of cosmic star formation. These galaxies form the most massive part of the galaxy population at these redshifts (Arcila-Osejo et al. 2019), and their extremely strong clustering suggests that they are associated with dark matter haloes that will grow into present-day massive galaxy clusters (Cheema et al. 2020).

Our analysis in this paper focused on the number of companions within 0.5 Mpc of our UMPEGs. In their deepest part, our data allow us to detect both quiescent and star-forming companions down to $M_\star^{\rm sat} \sim M_\star^*$, or a mass ratio of $M_\star^{\rm sat}:M_\star^{\rm UMPEG} \sim 1:7.5$; meanwhile, the wide area of the survey lets us apply a statistical fore/background correction to infer the number of physically associated massive satellites.

The main findings of our analysis are as follows:

(i) UMPEGs at $z \sim 1.6$ have very few companions of comparable mass: UMPEGs have virtually no massive physical companion galaxies (mass ratios $M_\star^{\rm sat} : M_\star^{\rm UMPEG} \gtrsim 1:3$), and on average have only one satellite per UMPEG down to mass ratio $M_\star^{\rm sat}:M_\star^{\rm UMPEG} \sim 1:5.5$.

(ii) Given this paucity of companions, there is at present no strong evidence from galaxy counts that UMPEGs reside in overdense regions. However, this is likely simply because our relatively shallow data do not probe sufficiently deep to find (lower-mass) satellites in significant numbers: in the Wide fields, where the bulk ($\sim$ 90 per cent) of our sample resides, we are complete to $M_\star \approx M_\star^* \approx 10^{10.7} {\rm M}_\odot$ and deeper data are needed to reach the bulk of the galaxy population at $M_\star \approx M_\star^*$ and below. Indeed, in the Deep fields (where we only have six UMPEGs given the small total area of these fields, but where we reach lower companion masses) such lower mass companions are seen, with a large luminosity (or

mass) gap between the UMPEG and their brightest (most massive) satellites.

(iii) The presence of the luminosity (mass) gap suggests that UMPEGs reside in environments that have formed significantly before we observe them at $z \sim 1.6$. In this scenario, dynamical friction leads to rapid merging of the most massive galaxies and leaves behind only lower mass satellites, which take longer to merge. This suggests that UMPEG progenitors may have assembled via major (mass ratio > 1:4) mergers at $z > 1.6$.

(iv) We estimate the UMPEG mass accretion rate due to mergers with satellites of mass ratio $M_\star^{\text{sat}} : M_\star^{\text{UMPEG}} > 1{:}4$ to be ~ 13 per cent Gyr^{-1} with a $\sim$factor of 2 systematic uncertainty. Projected back in time, the estimated growth rate suggests that at $z \sim 4$ the typical progenitor of a $z \sim 1.6$ UMPEG had a stellar mass of $\sim 10^{11.43} \text{M}_\odot$ (if that progenitor was star forming, its $z \sim 4$ mass would have been lower). Evolution from $z \sim 4$ to $z \sim 1.6$ could have been accomplished by major mergers, with typically a single major merger (as expected from the presence of the mass gap) with mass ratio of $\sim 2.7{:}1$ being enough to grow the mass to the $M_\star^{\text{UMPEG}} \sim 10^{11.57} \text{M}_\odot$ observed at $z \sim 1.6$. In addition to the presence of the mass gap, such early growth through major mergers is also supported by the fact that ~ 10 per cent of our original UMPEG candidates are double-cored and thus possibly undergoing mergers.

(v) Were the estimated merger rate continue to $z \sim 0$, then a typical UMPEG, with $M_\star^{\text{UMPEG}} \sim 10^{11.6} \text{M}_\odot$ at $z \sim 1.6$, would grow to $M_\star \sim 10^{12.0}$ through mergers with relatively massive companions. This projected $z \sim 0$ mass is consistent with the masses of present-day massive cluster BCGs lending further support to the idea (raised by Cheema et al. 2020) that UMPEGs are the direct, already-quiescent and massive progenitors of the central galaxies of some of the present-day massive galaxy clusters such as Virgo and Coma.

(vi) The estimated growth rate (~ 13 per cent Gyr^{-1}) is relatively mild and thus is unlikely to significantly affect the shape of the steep, exponential end of the galaxy stellar mass function of passive galaxies. Any such (minor) merger-induced change in M^* will be obscured by the addition of newly quenched massive galaxies, and the Schechter function of quiescent galaxies can be regarded as primarily a reflection of the mass-quenching process (Peng et al. 2010).

Overall, the results presented in this paper are consistent with the idea that $z \sim 1.6$ UMPEGs may be the direct, largely formed progenitors of some (~ 1-in-8; Cheema et al. 2020) of the central galaxies in present-day massive clusters. It seems plausible that galaxies that follow the UMPEG evolutionary pathway may grow through major mergers at very high redshifts, $z > 1.6$ before being observed as quiescent UMPEGs at $z \sim 1.6$, and then growing mildly mostly through minor mergers at lower redshifts.

A detailed understanding of how such progenitor galaxies already assembled and quenched by $z \sim 1.6$ remains a topic for further study, but our sample of high-z UMPEGs offers opportunities for such work through follow-up spectroscopy that can constrain their metallicities and, hence assembly pathways, and through deeper imaging that can probe for morphological evidence of merger events and search for fainter companions that could be used for halo occupation distribution (HOD) analyses.

REFERENCES

Abdurro'uf, Akiyama M., 2018, MNRAS, 479, 5083
Arcila-Osejo L., Sawicki M., 2013, MNRAS, 435, 845
Arcila-Osejo L., Sawicki M., Arnouts S., Golob A., Moutard T., Sorba R., 2019, MNRAS, 486, 4880
Belli S., Newman A. B., Ellis R. S., 2016, ApJ, 834, 18
Bertin E., Arnouts S., 1996, Astron. Astrophys. Suppl. Ser., 117, 393
Bielby R. et al., 2012, A&A, 545, A23
Blain A. W., Chapman S. C., Smail I., Ivison R., 2004, ApJ, 611, 725
Bridge C. R., Carlberg R. G., Sullivan M., 2010, ApJ, 709, 1067
Brodwin M. et al., 2008, ApJ, 687, L65
Burke C., Collins C. A., 2013, MNRAS, 434, 2856
Chabrier G., 2003, PASP, 115, 763
Chandrasekhar S., 1943, ApJ, 97, 255
Cheema G. K., Sawicki M., Arcila-Osejo L., Golob A., Moutard T., Arnouts S., Coupon J., 2020, MNRAS, 494, 804,
Contini E., De Lucia G., Hatch N., Borgani S., Kang X., 2016, MNRAS, 456, 1924
Cooke K. C., Kartaltepe J. S., Tyler K. D., Darvish B., Casey C. M., Le Févre O., Salvato M., Scoville N., 2019, ApJ, 881, 150
Daddi E., Cimatti A., Renzini A., Fontana A., Mignoli M., Pozzetti L., Tozzi P., Zamorani G., 2004, ApJ, 617, 746
Dariush A. A., Raychaudhury S., Ponman T. J., Khosroshahi H. G., Benson A. J., Bower R. G., Pearce F., 2010, MNRAS
De Lucia G., Blaizot J., 2007, MNRAS, 375, 2
Edwards L. O. V., Patton D. R., 2012, MNRAS, 425, 287
Forrest B. et al., 2020, ApJ, 890, L1
Fraser-McKelvie A., Brown M. J. I., Pimbblet K. A., 2014, MNRAS, 444, L63
Glazebrook K. et al., 2017, Nature, 544, 71
Goranova Y., Hudelot P., McCracken H. J., Mellier Y., 2010, The CFHTLS T0006 Release
Hartley W. G., Conselice C. J., Mortlock A., Foucaud S., Simpson C., 2015, MNRAS, 451, 1613
Hickox R. C. et al., 2012, MNRAS, 421, 284
Ilbert O. et al., 2013, A&A, 556, A55
Jiang C. Y., Jing Y. P., Faltenbacher A., Lin W. P., Li C., 2008, ApJ, 675, 1095
Johnston R., Vaccari M., Jarvis M., Smith M., Giovannoli E., Häußler B., Prescott M., 2015, MNRAS, 453, 2541
Jones L. R., Ponman T. J., Forbes D. A., 2000, MNRAS, 312, 139
Kado-Fong E. et al., 2017, ApJ, 838, 57
Kauffmann G., White S. D. M., 1993, MNRAS, 261, 921
Kawinwanichakij L. et al., 2014, ApJ, 792, 103
Kitzbichler M. G., White S. D. M., 2008, MNRAS, 391, 1489
Kubo M., Tanaka M., Yabe K., Toft S., Stockmann M., Gómez-Guijarro C., 2018, ApJ, 867, 1
Lidman C. et al., 2012, MNRAS, 427, 550

Lidman C. et al., 2013, MNRAS, 433, 825

Liu F. S., Mao S., Meng X. M., 2012, MNRAS, 423, 422

Liu F. S., Lei F. J., Meng X. M., Jiang D. F., 2015, MNRAS, 447, 1491

Lotz J. M. et al., 2008, ApJ, 672, 177

Marchesini D. et al., 2014, ApJ, 794, 65

Marsan Z. C. et al., 2019, ApJ, 871, 201

McDonald M. et al., 2016, ApJ, 817, 86

Milosavljević M., Miller C. J., Furlanetto S. R., Cooray A., 2006, ApJ, 637, L9

Moutard T. et al., 2016a, A&A, 590, A102

Moutard T. et al., 2016b, A&A, 590, A103

Munoz-Cuartas J. C., Maccio A. V., Gottlober S., Dutton A. A., 2011, MNRAS, 411, 584

Muzzin A. et al., 2013a, ApJ, 777, 18

Muzzin A. et al., 2013b, ApJS, 2068

Oke J. B., 1974, ApJS, 27, 21

Onodera M. et al., 2012, ApJ, 755, 26

Ostriker J. P., Tremaine S. D., 1975, ApJ, 202, L113

Patton D. R. et al., 2002, ApJ, 565, 208

Patton D. R., Carlberg R. G., Marzke R. O., Pritchet C. J., da Costa L. N., Pellegrini P. S., 2000, ApJ, 536, 153

Peng Y.-J. et al., 2010, ApJ, 721, 193

Ragone-Figueroa C., Granato G. L., Ferraro M. E., Murante G., Biffi V., Borgani S., Planelles S., Rasia E., 2018, MNRAS, 479, 1125

Raouf M., Khosroshahi H. G., Mamon G. A., Croton D. J., Hashemizadeh A., Dariush A. A., 2018, ApJ, 863, 40

Sawicki M., Yee H. K. C., 1998, AJ, 115, 1329

Shi K. et al., 2019, ApJ, 871, 83

Sorba R., Sawicki M., 2015, MNRAS, 452, 235

Sorba R., Sawicki M., 2018, MNRAS, 476, 1532

Stockmann M. et al., 2020, ApJ, 888, 4

Tal T., Wake D. A., van Dokkum P. G., van den Bosch F. C., Schneider D. P., Brinkmann J., Weaver B. A., 2012, ApJ, 746, 138

Tal T., van Dokkum P. G., Franx M., Leja J., Wake D. A., Whitaker K. E., 2013, ApJ, 769, 31

Toba Y. et al., 2017, ApJ, 835, 36

Tomczak A. et al., 2014, ApJ, 783, 85

Tremaine S. D., Richstone D. O., 1977, ApJ, 212, 311

Van Den Bosch F. C. et al., 2007, MNRAS, 376, 841

Veale M., Ma C.-P., Greene J. E., Thomas J., Blakeslee J. P., McConnell N., Walsh J. L., Ito J., 2017, The MNRAS, 471, 1428

Vulcani B. et al., 2016, ApJ, 816, 86

Whitaker K. E. et al., 2014, ApJ, 795, 104

White S. D. M., Frenk C. S., 1991, ApJ, 379, 52

White S. D. M., Rees M. J., 1978, MNRAS, 183, 341

Wilkinson A. et al., 2017, MNRAS, 464, 1380

Wright E., 2006, PASP, 118, 1711

Zhao D., Conselice C. J., Aragón-Salamanca A., Almaini O., Hartley W. G., Lani C., Mortlock A., Old L., 2017, MNRAS, 464, 1393

Zibetti S., Charlot S., Rix H.-W., 2009, MNRAS, 400, 1181

This paper has been typeset from a TEX/LATEX file prepared by the author.